Dimanganese(II) Accordion Porphyrin as a Functional Model for Catalases

Nikolay N. Gerasimchuk, Aida Gerges, Thomas Clifford, Andrew Danby, and Kristin Bowman-James*

Department of Chemistry, University of Kansas, Lawrence, Kansas 66045

Received March 11, 1999

Introduction

Interest in manganese enzymes has surged in recent years as a result of continuing efforts to understand their versatile chemistry.[1−5] Of these enzymes, the binuclear manganese catalases have been of particular focus in a number of groups. Catalases from *Thermus thermophilus*,[6] *Lactobacillus plantarum*,[7,8] and *Thermoleophilium album*[9] all contain dinuclear manganese centers which catalyze the disproportionation of H_2O_2 into H_2O and O_2. X-ray crystallographic results for manganese catalase from *T. thermophilus* indicate that the manganese ions are separated by ∼3.6 Å.[10] EPR[11−14] studies suggest the possibility of four oxidation state pairs: Mn_2(II/II), Mn_2(II/III), Mn_2(III/III), and Mn_2(III/IV), although the catalytic reaction most probably involves a cycling process between the Mn_2(II/II) and Mn_2(III/III) forms.[5] It is also believed on the basis of these studies that a μ-carboxylate, μ-hydroxo structure is involved. A number of models have been proposed for the manganese catalases, although the number of truly functional models has indeed been somewhat limited.[15−36]

Our interest in catalase models began as an offshoot to an ongoing project in our group involving expanded porphyrins.[37−41] During the course of our studies we obtained the crystal structure of the dimanganese(II) complex **1**. The key structural features

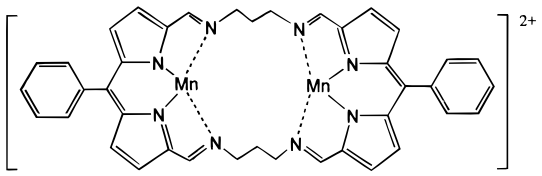

1

include both chelating and bridging carboxylates and a coordinated water molecule, features which are similar to those found for a number of bimetallic proteins. In further investigations **1** was found to exhibit catalase activity, with initial rates of O_2 evolution showing a dependence on the pK_a values of added nitrogenous bases. This model differs from a number of other functional model systems in that it does not contain μ-oxo linkages between the two metal ions built into the ligand framework. Herein are described both the crystal structure and results of studies of the catalase activity for **1**.

Experimental Section

Instrumentation. UV−vis spectra were recorded by means of Shimadzu SP2100 and HP diode array spectrophotometers in the range of 210−800 nm in quartz cuvettes of 0.1 and 1.0 cm at 290 K. X-band EPR spectra at 80 K (frozen glass) were recorded using a BRUKER cps300E FT spectrometer equipped with signal-channel and field controller blocks, at 25 dB attenuation and 0.63 mW microwave power,

(1) Christou, G. *Acc. Chem. Res.* **1989**, *22*, 328−335.
(2) Wieghardt, K. *Angew. Chem., Int. Ed. Engl.* **1989**, *28*, 1153−1172.
(3) Que, L., Jr.; True, A. E. *Prog. Inorg. Chem.: Bioinorg. Chem.* **1990**, *38*, 97−200.
(4) Manchanda, R.; Brudvig, G. W.; Crabtree, R. H. *Coord. Chem. Rev.* **1995**, *144*, 1−38.
(5) Dismukes, G. C. *Chem. Rev.* **1996**, *96*, 2909−2926.
(6) Barynin, V. V.; Grebenko, A. I. *Dokl. Acad. Nauk SSSR* **1986**, *286*, 461−464.
(7) Kono, Y.; Fridovich, I. *J. Biol. Chem.* **1983**, *258*, 6015−6019.
(8) Kono, Y. *J. Biol. Chem.* **1983**, *258*, 13646−13648.
(9) Algood, G. S.; Perry, J. J. *J. Bacteriol.* **1986**, *168*, 563−567.
(10) Barynin, V. V.; Vagin, A. A.; Melik-Adamyan, W. R.; Grebenko, A. I.; Khangulov, S. V.; Popov, A. N.; Andrianova, M. E.; Vainshtein, B. K. *Dokl. Acad. Nauk SSSR [Crystallogr.]* **1986**, *288*, 877−880.
(11) Fronko, R. M.; Penner-Hahn, J. E.; Bender, C. J. *J. Am. Chem. Soc.* **1988**, *110*, 7554−7555.
(12) Khangulov, S. V.; Barynin, V. V.; Antonyuk-Barynina, S. V. *Biochim. Biophys. Acta* **1990**, *1020*, 25−33.
(13) Pessiki, P. J.; Khangulov, S. V.; Ho, D. M.; Dismukes, G. C. *J. Am. Chem. Soc.* **1994**, *116*, 891−897.
(14) Khangulov, S. V.; Pessiki, P. J.; Barynin, V. V.; Ash, D. E.; Dismukes, G. C. *Biochemistry* **1995**, *34*, 2015−2025.
(15) Larson, E. J.; Pecoraro, V. L. *J. Am. Chem. Soc.* **1991**, *113*, 3810−3818.
(16) Larson, E. J.; Pecoraro, V. L. *J. Am. Chem. Soc.* **1991**, *113*, 7809−7810.
(17) Gelasco, A.; Askenas A.; Pecoraro, V. L. *Inorg. Chem.* **1996**, *35*, 1419−1420.
(18) Gelasco, A.; Kirk, M. L.; Kampf, J. W.; Pecoraro, V. L. *Inorg. Chem.* **1997**, *36*, 1829−1837.
(19) Gelasco, A.; Bensiek, S.; Pecoraro, V. L. *Inorg. Chem.* **1998**, *37*, 3301−3309.
(20) Wieghardt, K.; Bossek, U.; Nuber, B.; Weiss, J.; Bonvoisin, J.; Corbella M.; Vitols, S. E.; Girerd J. *J. Am. Chem. Soc.* **1988**, *110*, 7398−7411.
(21) Naruta, Y.; Sasayam, M *J. Chem. Soc., Chem. Commun.* **1994**, 2667−2668.
(22) Naruta, Y.; Maruyama, K. *J. Am. Chem. Soc.* **1991**, *113*, 3595−3596.
(23) Naruta, Y.; Sasayama, M. *Chem. Lett.* **1994**, 2411−2412.
(24) Wada, H.; Motoda, K.-I.; Ohba, M.; Sakiyama, H.; Matsumoto, N.; Okawa, H. *Bull Chem. Soc. Jpn.* **1995**, *68*, 1105−1114.
(25) Okawa, H.; Sakiyama, *Pure Appl. Chem.* **1995**, *67*, 273−280.
(26) Itoh, M.; Motoda, K.; Shindo, K.; Kamiusuki, T.; Sakiyama, H.; Matsumoto, N.; Okawa, H. *J. Chem. Soc., Dalton Trans.* **1995**, 3635−3641.
(27) Higuchi, C.; Sakiyama, H.; Okawa, H.; Fenton, D. E. *J. Chem. Soc., Dalton Trans.* **1995**, 4015−4020.
(28) Nagata, T.; Mizukami, J. *J. Chem. Soc., Dalton Trans.* **1995**, 2825−2830.
(29) Nagata, T.; Ikawa, Y.; Maruyama, K. *J. Chem. Soc., Chem. Commun.* **1994**, 431−432.
(30) Pessiki, P. J.; Khangulov, S. V.; Ho, D. M.; Dismukes, G. C. *J. Am. Chem. Soc.* **1994**, *116*, 891−897.
(31) Casey, M. T.; McCann, M.; Devereux, M.; Curran, M.; Cardin, C.; Convery, M.; Quillet, V.; Harding, C. *J. Chem. Soc., Chem. Commun.* **1995**, 771−772.
(32) McCann, M.; Casey, M.; Devereux, M.; Curran, M.; Cardin, C.; Todd, A. *Polyhedron* **1996**, *15*, 2117−2120.
(33) Devereux, M.; Curran, M.; McCann, M.; Casey, M.; McKee, V. *Polyhedron* **1996**, *15*, 2029−2033.
(34) Delroisse, M.; Rabion, A.; Chardac. F.; Tetard, D.; Verhlac, J.-B.; Fraisse, L.; Seris, J.-L. *J. Chem. Soc., Chem. Commun.* **1995**, 949−950.
(35) Nishida, Y.; Akamatsu, T.; Tsuchiya, K.; Sakamoto, M. *Polyhedron* **1994**, *13*, 2251−2254.
(36) Tanase, T.; Lippard, S. J. *Inorg. Chem.* **1995**, *34*, 4682−4690.
(37) Acholla, F. V.; Mertes, K. B. *Tetrahedron Lett.* **1984,** *25*, 3269−3270.
(38) Acholla, F. V.; Takusagawa, F.; Mertes, K. B. *J. Am. Chem. Soc.* **1985**, *107*, 6902−6908.
(39) Acholla, F. V.; Mertes, K. B. *Bull. Chem. Soc. Ethiop.* **1988**, *2*, 73−78.
(40) Acholla, F. V.; Mertes, K. B. *Bull. Chem. Soc. Ethiop.* **1989**, *3*, 17−24.
(41) Reiter, W. A.; Gerges, A.; Lee, S.; Deffo, T.; Clifford, T.; Danby, A.; Bowman-James, K. *Coord. Chem. Rev.* **1998**, *174*, 343−359. (This reference includes a preliminary structural report for **1**.)

10.1021/ic990576t CCC: $18.00
Published on Web 11/09/1999

Scheme 1

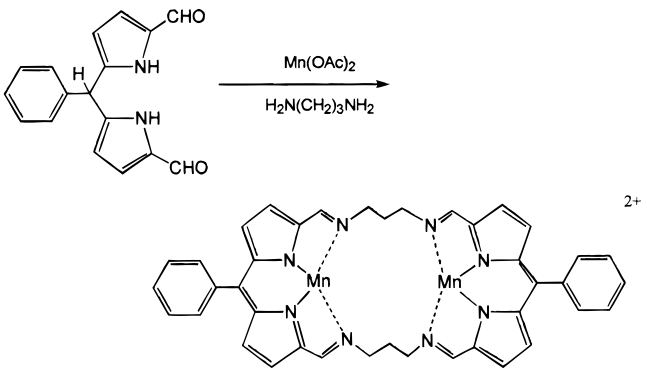

Table 1. Crystallographic Data for **1**·OAc_2·H_2O

empirical formula	$Mn_2C_{44}H_{42}N_8O_5$	V, Å^3	8235(5)
fw	872.74	Z	8
color, habit	red-violet, plate	ρ_{calcd}, g cm^{-1}	1.408
cryst dimens, mm	0.30 × 0.20 × 0.03	λ, Å	1.54178
space group	*Pbca*	μ, mm^{-1}	54.63
a, Å	26.614(4)	T, °C	23
b, Å	17.905(3)	R	0.078
c, Å	17.281	R_w	0.090

with a modulation amplitude of 10 G, a modulation frequency of 100 kHz, and a sweep width of 5000 G.

Synthesis. 2,2′-Benzyl-5,5′-diformyldipyrrole was prepared from pyrrole-2-carboxyaldehyde using a cyanovinyl protecting group[42] as reported earlier.[41] The complex was prepared from a Schiff base condensation between the dipyrrometh*ane* dialdehyde and 1,3-diaminopropane in the presence of manganese(II) acetate as template.[41] The resulting ligand is in the oxidized dipyrrometh*ene* form (Scheme 1).

Catalytic Studies. A sample of the complex **1** (1.50−2.50 mg, ∼10^{-3} mmol) was dissolved in ethanol (2 mL), and an aliquot of H_2O_2 (0.10 mL of a 45% solution, 1.44 mmol) was added. Amines were added in 0.144 mmol amounts and were obtained from stock solutions, which were made up from either freshly distilled or recrystallized amine. The evolution of O_2 was monitored volumetrically at 295 K, and initial rates were determined from the amount of O_2 evolved over the first minute. The maximum volume of O_2 produced from a 0.10 mL sample of the H_2O_2 solution was checked periodically by the standard reaction of H_2O_2 decomposition catalyzed by finely dispersed MnO_2. The concentration of H_2O_2 was determined by means of a Ce(IV) titration using $Fe(phen)_3^{3+}$ as the end point indicator.

Crystal Structure Data. Crystal structure data are provided in Table 1. A tiny crystal (0.30 × 0.20 × 0.03 mm) was chosen and mounted on a glass fiber. All measurements were made on a Rigaku AFC5R diffractometer with graphite-monochromated Cu Kα radiation and a 12 kW rotating anode generator. Cell constants and an orientation matrix for data collection were obtained from a least-squares refinement using the setting angles of 12 carefully centered reflections in the range 65° < 2θ < 70°. Preliminary measurements showed orthorhombic symmetry, and systematic absences 0kl, $k = 2n + 1$, $h0l$, $l = 2n + 1$, and $hk0$, $h = 2n + 1$ indicated the space group *Pbca* (no. 61). The data were collected at 23 °C using an $\omega-2\theta$ scan technique to a maximum 2θ of 112.7° for a total of 6016 reflections. The intensities of three representative reflections monitored after every 150 reflections remained constant throughout data collection. An empirical absorption correction was applied, which resulted in transmission factors ranging from 0.84 to 1.34, using the program DIFABS,[43] and the data were also corrected for Lorentz and polarization effects. The structure was solved by direct methods.[44] The non-hydrogen atoms were refined anisotropically, and the final cycle of full-matrix least-squares refinement was based on 2769 observed reflections ($I > 1.00\sigma(I)$) and 532 variable parameters, and converged (the largest parameter shift was 0.08 times its esd) with unweighted and weighted agreement factors of $R = \sum||F_o| - |F_c||/\sum|F_o| = 0.078$ and $R_w = [(\sum w(|F_o| - |F_c|)^2/\sum wF_o^2)]^{1/2} = 0.090$. The standard deviation of an observation of unit weight was 1.17. Neutral atom scattering factors were taken from Cromer and Waber.[45] Anomalous dispersion effects were included in F_c;[46] the values for $\Delta f'$ and $\Delta f''$ were those of Cromer.[47] All calculations were performed using the TEXSAN crystallographic software package of Molecular Structure Corp.[48] Table 2 lists bond lengths of interest around the two metal coordination spheres. Listings of final positional and thermal parameters (including hydrogen atoms) and a complete set of bond lengths and angles are available as Supporting Information.

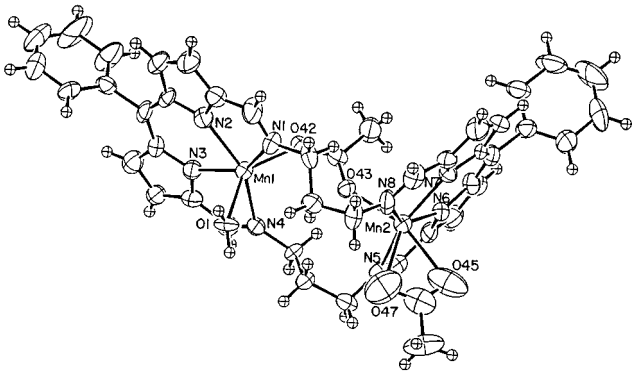

Figure 1. ORTEP view of **1** showing the numbering scheme of the coordination sphere.

Table 2. Intramolecular Distances (Å) for the Metal Coordination Spheres for **1**·OAc_2·H_2O

atoms	distance	atoms	distance
Mn(1)−N(1)	2.493(9)	Mn(2)−N(5)	2.41(1)
Mn(1)−N(2)	2.227(9)	Mn(2)−N(6)	2.225(9)
Mn(1)−N(3)	2.225(9)	Mn(2)−N(7)	2.235(9)
Mn(1)−N(4)	2.474(9)	Mn(2)−N(8)	2.45(1)
Mn(1)−O(1)	2.162(7)	Mn(2)−O(43)	2.189(8)
Mn(1)−O(41)	2.102(7)	Mn(2)−O(45)	2.42(1)
		Mn(2)−O(47)	2.40(1)

Results and Discussion

Crystal Structure of the Dimanganese Complex 1. The macrocycle is in the dipyrromethene form, which means that the diformyldipyrromethane reactant oxidizes during the course of the Schiff base reaction. Upon complex formation, two of the pyrrole nitrogens deprotonate (much like the case in porphyrins) resulting in a dianionic ligand. The crystal structure of the acetate salt (Figure 1) reveals a dinuclear metal site with a Mn−Mn separation of 5.40 Å. Each dipyrromethane fragment is coordinated to a manganese ion in a planar fashion (Table 3), and the two planes are almost perpendicular to each other (Figure 2A). One of the acetate counterions forms a *cis,anti* bridge between the two metal ions, while the other is weakly chelated to one of the manganese(II) ions (Mn(2)−O = 2.42(1) and 2.40(1) Å) (Figure 2B and Table 2). Additionally, one water molecule is bound (Mn(1)−O(1) = 2.162(7) Å). Mn(1) thus maintains a distorted octahedral geometry, and Mn(2) forms a distorted pseudo-seven-coordinate complex.

(42) Paine, J. B., III; Dolphin, D. *J. Org. Chem.* **1988**, *53*, 2787−2795.
(43) Walker, N. P. C.; Stuart, D. I. *Acta Crystallogr.* **1983** *A39*, 158−166.
(44) Direct methods used were MITHRIL (Gilmore, C. J. *J. Appl. Crystallogr.* **1984**, *17*, 42) and DIRDIF (Beurskens, P. T. Technical Report Crystallography Laboratory, Toernooiveld, 6525 E. Nijmegen, The Netherlands, 1985).
(45) Cromer, D. T.; Waber, J. T. *International Tables for X-ray Crystallography*; Kynoch Press: Birmingham, 1974; Vol. IV, Table 2.2A.
(46) Ibers, J. A.; Hamilton, W. C. *Acta Crystallogr.* **1964**, *17*, 781−782.
(47) Cromer, D. T. *International Tables for X-ray Crystallography*, Kynoch Press: Birmingham, 1974; Vol. IV, Table 2.3.1.
(48) TEXSAN-TEXRAY Structure Analysis Package, Molecular Structure Corp., 1985.

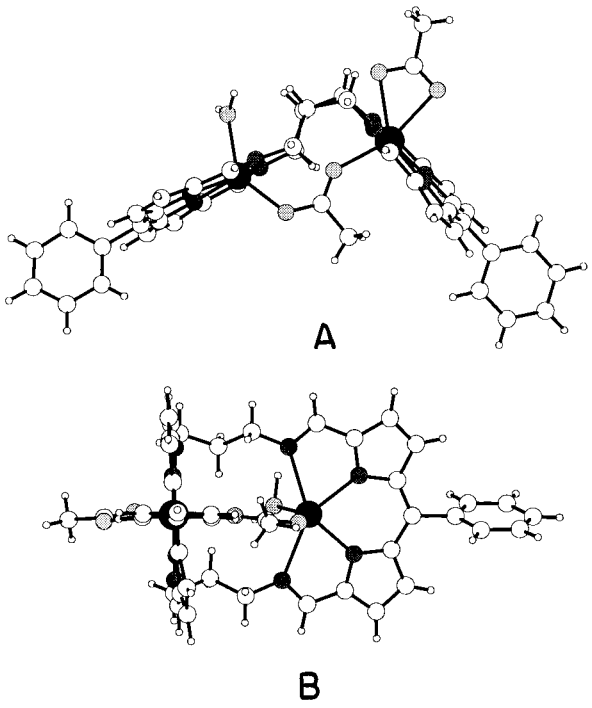

Figure 2. Two views of the coordination environments surrounding the manganese centers: (A) side view clearly showing the *cis,anti* conformation of the bridging acetate, along with the chelated acetate and water molecule; (B) overhead view showing the almost perpendicular orientation of the two dipyrromethane planes.

Table 3. Selected Least-Squares Planes and Atom Displacements for **1**·OAc_2·H_2O

atom	distance, Å	atom	distance, Å
	A. Mn(1)−N(1)−N(2)−N(3)−N(4)		
	$0.695x + 0.613y - 0.379z = -1.557$		
Mn(1)	0.047	N(3)	−0.047
N(1)	−0.046	N(4)	0.010
N(2)	0.036		
	B. Mn(2)−N(5)−N(6)−N(7)−N(8)		
	$0.662x - 0.580y + 0.466z = -2.982$		
Mn(2)	0.029	N(7)	0.043
N(5)	0.016	N(8)	−0.035
N(6)	−0.053		

Under closer scrutiny the coordination environment formed by the macrocycle is rather unusual. Only the pyrrole nitrogen atoms are coordinated with bond lengths anticipated for normal Mn(II)−N distances, with $Mn-N_{pyrrole}$ averaging 2.23 Å (Table 2). The imine nitrogens are only weakly associated, at distances between 2.4 and 2.5 Å. The fact that the imines display such weak interactions with the two metal ions is indicative of the strain imposed by the four-membered chelate rings ($N_{pyrrole}$=C−CH=N_{imine}).

The presence of both bridging and chelated acetates as well as the bound water molecule renders the complex structurally similar to that found in a number of binuclear protein sites,[1−5] with the exception of the rather long Mn−Mn distance. The role of coordinated carboxylates and possible changing binding modes (a "carboxylate shift")[49] during the catalytic act in metalloproteins has been the subject of considerable discussion.[1−5,49] The presence of the loosely chelated as well as the coordinated acetate in this catalase model and the possibility of carboxylate shifts during reaction sequences may be factors which facilitate the observed reactivity.

(49) Rardin, R. L.; Tolman, W. B.; Lippard, S. J. *New J. Chem.* **1991**, *15*, 417−430.

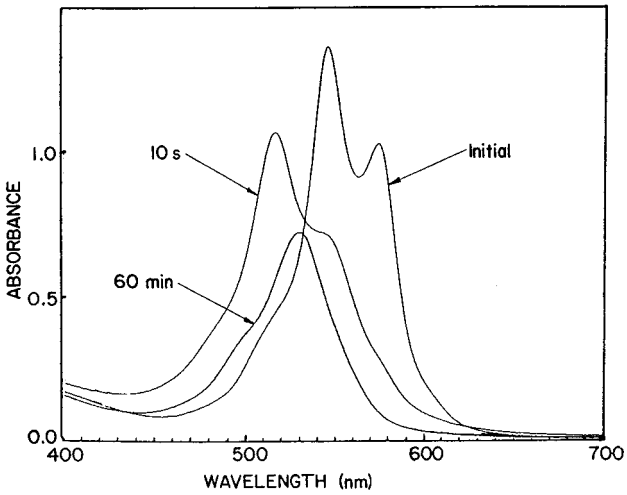

Figure 3. UV−vis spectra of **1** shown at three time intervals. The solution contains a 1:4 molar ratio of **1**:H_2O_2 in ethanol.

Catalase Activity. The acetate salt of **1** reacts with H_2O_2, leading to the evolution of O_2. During the reaction the UV−vis spectrum changes significantly (Figure 3), with absorptions at 546 nm ($\epsilon = 28\,800$) and 574 nm ($\epsilon = 23\,400$) being replaced by a single absorption band at 510 nm. This change is similar to that observed when H_2O is added to an alcoholic solution of **1**.[41] While the spectral changes are not clearly understood, they may be related to H_2O or H_2O_2 binding to the manganese with a concomitant alteration of the metal ion coordination mode. As a case in point, the crystal structure of the diazido salt of a related copper(II) "accordion porphyrin" complex indicates a very different coordination geometry with *endo/exo* orientations of the imines and no coordinated solvent.[38]

Under catalytic conditions, the reaction of the acetate salt of **1** with H_2O_2 begins immediately upon addition of the substrate. The reaction proceeds with an initial rate of O_2 evolution of 0.07 mL of O_2 s^{-1}. There is no lag time at the onset of the reaction, indicating that the complex, as opposed to a decomposition product, is responsible for the disproportionation. (It should be noted that, in some manganese catalase models, MnO_2 has been identified as the actual catalyst.[36]) Flaky precipitates form during the reaction, which are thought to be a mixture of the free ligand and other decomposition products. These precipitates readily dissolve in DMF and show no catalytic activity. This decomposition occurs within about 30 min.

When triethylamine is added, the initial rate of O_2 evolution accelerates to 0.23 mL of O_2 $s.^{-1}$ Such a finding is not surprising since a base-catalyzed mechanism has been postulated for the catalases.[1−5] Similar findings of base accelerations have been observed for other model compounds.[15−19,21−23,31−33] However, systematic studies of the influence of added base have been rather limited.[23] To explore the influence of base on the reaction, a series of six amines were chosen: quinoline, pyridine, morpholine, imidazole, hydrazine, and triethylamine, as representative bases with pK_a values ranging from 5 to 11. Using a ratio of H_2O_2:amine:complex = 1000:100:1, a distinct correlation between the pK_a of the amine and the amount of O_2 produced during the first 20 min of the reaction was found (Figure 4). Triethylamine, the base with the highest pK_a value at 10.71, provided the greatest initial rate acceleration as well as the largest volume of O_2 produced (14.46 mL). It is generally believed that the influence of base in the enzymes most probably derives from a general-base catalysis, i.e., assisting in the deprotonation of the H_2O_2 substrate.[1] The active base in the catalases is proposed to have a pK_a of ∼5.5,[5] which could

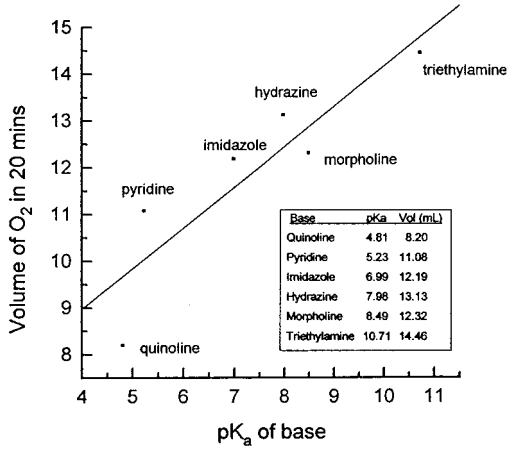

Figure 4. Correlation between the pK_a of added base and the volume of O_2 evolved (mL) during the first 20 min of reaction.

explain why quinoline, with a pK_a of 4.81,[50] falls off the otherwise ascending scale so dramatically.

Nitrogenous and other bases containing oxygen are also capable of coordination to the metal ions in these types of systems. A systematic study of the influence of both types of bases in manganese and iron porphyrins indicated that the donor atom can play a major role in the propensity of the complex to catalyze both dismutation and oxygenation reactions.[51] For the manganese accordion porphyrin **1**, however, there is virtually no spectroscopic change in the electronic spectrum upon the addition of the bases. This finding leads us to believe that the base does not coordinate to either of the metal ions. However, the presence of the coordinated water molecule found in the crystal structure leads to another mechanistic possibility. It is entirely possible that the base could additionally (or instead) provide for a conjugate base, S_N1_{CB}, mechanism by deprotonating the coordinated water molecule. If this were the case, it could result in labilizing the *trans*-bound acetate, thus freeing up a coordination site, and facilitating H_2O_2 binding. At this point it is not possible to discriminate between the two mechanisms, and both may be operating.

Conclusions

The accordion-like tetrapyrrolic manganese(II) complex **1** has been found to catalyze the disproportionation of H_2O_2, making it a new functional model for dimanganese catalases. The presence of both coordinated and weakly chelated acetates and additionally a coordinated water molecule makes the coordination environment surrounding the two manganese ions similar to that in a number of bimetallic enzymes. In addition, the bound water molecule may provide assistance via a S_N1_{CB}-type mechanism, labilizing the bridging acetate and freeing up a coordination site for the H_2O_2. Explorations are underway to identify other biomimetic roles for complexes with this and related tetrapyrrolic ligands.

Acknowledgment. This work was funded by the National Institutes of Health Grant GM 37577, the American Heart Association Grant KS-93-GS-38, and the National Science Foundation EPSCoR Program. We also acknowledge helpful discussions with Professor Colin Cairns. The crystal structure was determined at the X-ray Crystallography Laboratory at the University of Kansas by Dr. Fusao Takusagawa and Larry Seib, and their assistance is also appreciated.

Supporting Information Available: X-ray crystallographic data. This material is available free of charge via the Internet at http://pubs.acs.org.

IC990576T

(50) pK_a values were obtained from Smith, R. M.; Martell, A. E. *Critical Stability Constants*; Plenum Press: New York, 1975; Vol. 2, Amines (quinoline, pyridine, imidazole, morpholine, and triethylamine); Vol. 4, Inorganic Complexes (hydrazine).

(51) Robert, A.; Loock, B.; Momenteau, M.; Meunier, B. *Inorg. Chem.* **1991**, *30*, 706−711.